CONF-970201--26

FeAl-TiC and FeAl-WC Composites - Melt Infiltration Processing, Microstructure and Mechanical Properties

R. Subramanian and J.H. Schneibel
Metals and Ceramics Division
Oak Ridge National Laboratory

ABSTRACT:

TiC-based and WC-based cermets were processed with iron aluminide, an intermetallic, as a binder by pressureless melt infiltration to near full density (> 97 % theoretical density). Phase equilibria calculations in the quaternary Fe-Al-Ti-C and Fe-Al-W-C systems at 1450 °C were performed to determine the solubility of the carbide phases in liquid iron aluminide. This was done by using Thermocalc™ and the results show that molten Fe-40 at. % Al in equilibrium with $Ti_{0.512}C_{0.488}$ and graphite, dissolves 4.9 at. % carbon and 64 atomic ppm titanium. In the Fe-Al-W-C system, liquid Fe-40 at. % Al in equilibrium with graphite dissolves about 5 at. % carbon and 1 at. % tungsten. Due to the low values for the solubility of the carbide phases in liquid iron aluminide, liquid phase sintering of mixed powders does not yield a dense, homogenous microstructure for carbide volume fractions greater than 0.70. Melt infiltration of molten FeAl into TiC and WC preforms serves as a successful approach to process cermets with carbide contents ranging from 70 to 90 vol. %, to greater than 97 % of theoretical density. Also, the microstructures of cermets prepared by melt infiltration were very homogenous. Typical properties such as hardness, bend strength and fracture toughness are reported. SEM observations of fracture surfaces suggest the improved fracture toughness to result from the ductility of the intermetallic phase. Preliminary experiments for the evaluation of the oxidation resistance of iron aluminide bonded cermets indicate that they are more resistant than WC-Co cermets.

1. INTRODUCTION:

TiC-Ni cermets and WC-Co cemented carbides or the so-called "hard metals" are both composites with more than 60 volume % of the carbide phase bound by a metallic phase (Co or Ni), which exhibit attractive mechanical properties making them indispensable in a variety of industrial applications [1]. However, over the last few decades, significant research effort has gone into identifying alternate binders for the cermets in order to improve their mechanical properties and also to overcome some shortcomings, namely, poor corrosion resistance, high cost and environmental toxicity [2-6]. Iron, cobalt and nickel-based alloys were found to be suitable binders for WC-based cermets by various investigators [2-5] due to their excellent wetting of the carbide phases and also, solubility of the carbide phases in the molten binder. Viswanadham et al. [4,5] processed (Fe,Ni,C)-WC cermets and studied the effect of martensitic transformations in the (Fe,Ni,C) binder alloys on the fracture toughness of the cermets.. Research by Almond and Roebuck [2,3] demonstrated the feasibility of processing WC-Ni cermets. However, their fracture toughness and strength were evaluated to be lower than those of WC-Co cermets. Modification of the binder properties by addition of aluminum to form γ' precipitates raised the strength but decreased the fracture toughness [5]. Optimization of the binder composition in TiC-Ni cermets was also performed to obtain superior mechanical properties [6].

Recently, intermetallics, such as iron aluminides and nickel aluminides, have shown to be successfully used as a binder in the TiC and WC-based cermets [7-9]. Aluminides, especially iron-based, are known to be extremely resistant to corrosion under sulfidizing atmospheres, oxidizing atmospheres and in molten salts [10-12]. Aluminides can form an impervious

DISCLAIMER

aluminum oxide layer easily and this can provide excellent corrosion resistance in a wide range of corrosive environments [10,12]. Thus intermetallic-carbide and intermetallic-boride composites are expected to possess a good combination of high wear resistance and corrosion resistance. Some of the composites that have been processed by liquid phase sintering of mixed powders to nearly full density include ceramics such as TiC, WC, TiB_2 and ZrB_2 bonded by iron aluminide [7,8] and Ni_3Al-bonded TiC and WC [9].

Although the formation of an impervious alumina layer is beneficial for the final composite, it becomes an obstacle during the processing of these cermets by traditional liquid phase sintering techniques. As shown in this study, liquid phase sintering of a mixture of fine iron aluminide powders (with an oxide layer) and carbide particles to process cermets, with greater than 70 vol. % carbide phase, leads to composites with an inhomogenous microstructure and low density. Melt infiltration of carbide preforms has been shown to successfully overcome these issues and allows processing of intermetallic aluminide bonded WC and TiC-based cermets [13-15].

Processing of materials by melt infiltration has been demonstrated for many systems, beginning with the manufacturing of cupric steel parts obtained by infiltrating porous iron bodies by molten Cu [16]. Spontaneous infiltration of the preform occurs mainly due to excellent wetting of the molten metal and a capillary force due to the pores in the preform. An additional feature of this process is a minimum chemical reaction without the formation of new reaction products. Spontaneous infiltration has been used for the processing of many metal matrix composites [17-19]. In the absence of good wetting, external pressure delivered by a gas or a mechanical device is used to obtain full density of the composite. This principle is used in the processing of composites by squeeze casting, such as Al/SiC composites [20] and also, ceramic matrix composites, such as, Al_2O_3/Ni_3Al [21]. But, application of external pressure increases the complexity and consequently, the cost of the process. Another infiltration technique utilizes the reaction between the melt and the preform, thus eliminating the need for an external pressure. This approach, known as reactive infiltration, has been very well demonstrated in the processing of siliconised SiC [22,23] and also, recently for many other systems such as, reaction between Al and AlN [24], Al and Mullite [25] and formation of "C-4 composites" by reaction between aluminum and quartz [26]. Of the three possible methods of processing of composites by melt infiltration - non-reactive spontaneous, pressure assisted and reactive infiltration, the simplest is the processing approach by non-reactive spontaneous infiltration. Material combinations, with useful applications, which satisfy the requirements for spontaneous infiltration are few, but the processing of intermetallic bonded carbide and boride based cermets fall in this category.

In this paper, the ease of processing of cermets by melt infiltration to nearly full density is demonstrated. These results are supported by SEM observations of the microstructures and density measurements. Also, with FeAl bonded TiC as an example, important issues related to the melt infiltration technique, such as the wetting behavior, preform density and solubility limits of TiC in liquid iron aluminide are discussed. Typical mechanical properties such as fracture toughness, hardness and bend strength are presented. Reasons for the high fracture toughness are suggested based on the fracture surface observations of the cermets.

2. EXPERIMENTAL DETAILS

The starting materials used for processing of the composites were TiC powder (2-3 μm, Kennametal, Inc.), WC (Teledyne, 2.8 μm) and pre-alloyed Fe-40 at. % Al (-325 mesh, Homogenous Metals Inc.). The TiC powder had a combined carbon content of 19.45 wt % and a free carbon content of 0.1 wt %. The carbide powder was uniaxially cold pressed at 34 MPa. The green pellet was placed in an alumina dish with an appropriate amount of the iron aluminide powder, corresponding to the desired volume fraction, on the top surface of the

pellet. The furnace was maintained under a dynamic vacuum of about 10^{-4} Pa and the infiltration was carried out at a temperature of 1450 °C. The sample was held at this temperature for an hour allowing sufficient time for sintering after the initial infiltration. After cooling, specimens were cut, polished and examined with an optical microscope and a Hitachi-S4100 scanning electron microscope (SEM). Densities of the specimens were measured by the Archimedes immersion technique. Specimens for bend tests and fracture toughness measurements were electro-discharge machined and ground into bars with dimensions of 3 x 4 x 21 mm and finally polished with 3 μm diamond paste. Bend tests were performed at room temperature using a 3-point bend testing set-up with a span of 20 mm. The testing was performed in an Instron 4501 testing machine with a crosshead speed of 10 μm/sec. Chevron-notched specimens were also tested in the same set-up and the fractured surfaces were observed using a SEM. Rockwell hardness (R_A) of the composites was determined using a Wilson hardness tester and the Vickers hardness was measured with a load of 500 g and a dwell time of 15 seconds. The oxidation resistance of the cermets were determined by weight gain of the composites after exposure to air at 900 °C for 24 hours.

To determine the effect of the preform density on the final density of TiC-FeAl cermets, TiC preforms with 60 %, 70 % and 80 % theoretical density were prepared before infiltration. The differences in the densities were obtained by compacting the powders to various green densities and subjecting them to a simple sintering cycle. For the preforms with 60 % and 70 % of the theoretical density, the sintering cycle involved a degassing step at 1200 °C for 0.5 hour and raising the temperature to 1450 °C for approximately 1 minute. Starting with a bed of loose TiC powder, the above sintering cycle results in a 60 % dense preform whereas uniaxial compaction to 14 MPa, prior to sintering, results in a 70 % dense preform. Uniaxial compaction to 34 MPa (prior to sintering) and with a sintering sequence of 1200 °C for 0.5 hour and 0.5 hour at 1500 °C, results in a preform of about 80 % of the theoretical density. Appropriate amounts of the iron aluminide powder were weighed out and placed on top of the preforms, which were heated above the melting point of the iron aluminide, to 1450 °C, for infiltration. The samples were held at that temperature for 15 minutes. After a furnace cool, the densities of the cermets were determined and correlated to the volume fraction of the binder and the initial preform density.

3. RESULTS AND DISCUSSION

3.1. Fe-Al-Ti-C and Fe-Al-W-C Phase Equilibria At 1450 °C:

For an understanding of the processing of iron aluminide bonded TiC-based cermets by liquid phase sintering, an idea about the solubility of TiC in liquid iron aluminide is essential. This information can be obtained by performing calculations using Thermocalc™, a program which allows a determination of the composition of the phases in equilibrium (tie-lines) by minimizing the free energy of a system containing liquid iron aluminide (Fe-40 at. % Al, in our case) and TiC (or WC) at 1450 °C. The accuracy of the calculated phase stability limits depends on the extent of information available in the thermodynamic database regarding properties of the binary, ternary and quaternary compounds and solid solutions.

For the Fe-Al-Ti-C system, prediction of the binary phase diagrams Ti-C, Fe-Al, Al-Ti and Al-C accurately reproduced the experimentally known stability limits. For carbon containing ternary phase diagrams - Fe-Al-C, Ti-Al-C and Fe-Ti-C - isothermal sections at 1450 °C were not available and a comparison could be done only for selected isothermal sections, such as, 1300 °C for Ti-Al-C, 1300 °C for Fe-Al-C and 1500 °C for Fe-Ti-C. Results from the Thermocalc™ program agreed exactly with those published in the literature [27-30]. Prediction of phase stability limits in quaternary systems, such as Fe-Al-Ti-C, require an accurate extrapolation of the excess parameters (describing the non-ideality of the solid solutions) from the binary and ternary phase diagrams. This is achieved by a Redlich-Kister-Muggianu model in

Thermocalc™ [31]. No parameters were changed to obtain the final isothermal section at 1450 °C. At present, no phase diagrams or isothermal sections for the Fe-Al-Ti-C system at 1450 °C are available for comparison. The results from the calculation are shown in Fig. 1. It is evident that the solubility of TiC in liquid Fe40Al depends on the concentration of titanium and carbon in the liquid. The concentrations of Ti and C are inversely proportional to each other. In other words, with increasing Ti in the liquid, the carbon concentration decreases. This is due to a strong interaction between carbon and titanium in the liquid intermetallic, also observed in Fe-Ti-C system [32]. The thermodynamics of the variation in the solubility limit has been discussed in detail in the literature [32]. From Fig. 1, it is clear that the composition of TiC in equilibrium with the titanium and carbon in the liquid intermetallic varies over a large range. At the three-phase equilibrium, graphite and iron aluminide with 4.9 at. % carbon and 64 atomic ppm Ti are in equilibrium with $Ti_{0.512}C_{0.488}$. With an increase in titanium in liquid iron aluminide to 9.3 at. %, the carbon content drops to 57 atomic ppm and this composition is in equilibrium with $Ti_{0.575}C_{0.425}$. From the supplier's specifications, the stoichiometry of the TiC powder was $Ti_{0.511}C_{0.489}$, almost equal to the stoichiometry of TiC at the three-phase equilibrium. The solubility values are very low compared to the solubility of TiC in nickel, which is a commonly used binder in commercially available TiC-based cermets. Molten Ni, at 1460 °C, can dissolve 12 at. % of titanium and carbon [33]. This high solubility aids in the processing of the cermets by traditional liquid phase sintering of mixed powders and as presented in the following sections, iron aluminide bonded TiC-based cermets cannot be processed by such a process due to the lower solubility of TiC in iron aluminide.

The results from the calculations in the Fe-Al-W-C system are shown in Fig. 1b. The solubility of carbon is 5 at. % and that of tungsten is 1 at. % at the three phase equilibrium of WC, graphite and liquid iron aluminide. The carbon concentration decreases with an increase in the W content, although not as significantly as in Fe-Al-Ti-C system. WC is in equilibrium with W_2C at a concentration of 4 at. % W and 1 at. % carbon in molten iron aluminide. These values are significantly lower than those observed for the WC-Co system. Above the melting point of Co, at 1500 °C, almost 15 at. % W and 12 at. % C can be dissolved [34]. In addition, the presence of an eutectic at a lower temperature (1280 °C) aids in the early dissolution of the carbide phase, consequently leading to successful liquid phase sintering of mixed powders of WC and Co [1].

3.2. Wetting of TiC by liquid Fe40Al:

Figure 2 illustrates a low "contact" angle, an indication of good wetting of TiC (97 % dense) by liquid Fe40Al, after holding it for 15 minutes at 1450 °C. A complicating factor is the changing volume of the droplet, due to an infiltration of a part of the melt into the polycrystalline substrate along the grain boundaries. A single crystal substrate would have to be used to prevent the infiltration. In addition, the value of the contact angle is expected to change with time as shown by Aksay et. al. [35]. Change in the contact angle is possible depending upon the extent of chemical equilibration attained between the liquid and the substrate. A reaction between aluminum in the iron aluminide and oxygen present as a contaminant on TiC could also affect the contact angle. This effect has been discussed in detail by Muscat and Drew [36] during their systematic study of the infiltration of TiC by molten aluminum.

From the simple experiment described above, it was found that the composition of the alloy significantly affects the infiltration depth of iron aluminide into the dense polycrystalline substrate. Changes in the alloy composition by additions of 5 and 10 at. % Ti have shown that the depth of infiltration increases with the increase in Ti content. It is reasonable to assume that the capillary pressure is negligible due to the high density of the substrate (97 % dense). Therefore, the differences in the depth are very likely due to a reaction between Ti in the alloy and TiC. EDS analysis of the intermetallic phase along the grain boundaries shows that the Ti content in the infiltrated intermetallic is about 2 at. %, after infiltration of liquid

$Fe_{0.57}Al_{0.38}Ti_{0.05}$. The following reaction could have resulted in the final composition and also aided in the larger infiltration depth:

$Ti_{0.511}C_{0.489} + Fe_{0.57}Al_{0.38}Ti_{0.05} \rightarrow 1.029Ti_{0.525}C_{0.475} + 0.969\ Fe_{0.588}Al_{0.372}Ti_{0.02}$ (with 220 at. ppm C in solution)

The above reaction is intended only to illustrate a reaction due to change in stoichiometry of TiC. When 2 at. % Ti is present in the binder phase, only 220 at. ppm carbon is predicted (from Thermocalc™) to be dissolved in the intermetallic phase. The change in stoichiometry of the TiC grains could not be determined using the SEM. TEM analysis of the composition of the grains would be necessary to determine the stoichiometry and also to precisely determine the composition of the intermetallic. Similar experiments. with other alloying additions. such as W. Mo and C also show an effect on the infiltration depth and they are reported in Table 1.

Table 1: Effect of alloying additions on the infiltration depth of Fe40Al into a TiC substrate (97 % dense)

Alloying Additions	Infiltration Depths (μm)
None	100
3.5 wt. % C	100
5 at. % Ti	230
10 at. % Ti	650
5 at. % Mo	600
5 at. % W	450

Additions of Mo and W also aid the infiltration of the melt due to a reaction between the alloying additions and TiC to form a mixed carbide. These mixed carbides generally exhibit a core-rim effect as reported by Moskowitz and Humenik [37]. Addition of carbon does not show a similar effect which is possibly due to a lack of reaction between the alloy and substrate. To identify the effect of the alloying additions on the wetting of TiC, systematic wetting experiments on single crystal substrates would be required.

3.3. Effect of Preform density on the final density of the cermet:

From the simple relation suggested by Washburn [38], the rate of infiltration of liquids into a porous body is proportional to the pore radius, contact angle and surface tension and inversely proportional to the viscosity. Many modifications to the Washburn relation have emphasized the importance of the tortuosity of the pores and also an unstable contact angle due to a dynamic mass transfer between the preform and the infiltrating liquid [17,39]. The degree of sintering of the preform changes the capillary radius and the extent of the carbide-to-carbide contact and, therefore, the preform density is expected to affect the final density of the cermet.

Many infiltration processes use a pre-sintered preform with about 30 % porosity which is dipped in molten metal to fill up the pores by spontaneous infiltration. In the process described in this paper, a calculated amount of the infiltrant is placed on top of the substrate, which upon infiltration then results in densification, due to a rearrangement of the particles in the preform, similar to the step in a traditional liquid phase sintering process. A simple test of the effect of the preform density on the final density of the cermet suggests that an optimum preform density prior to infiltration leads to a maximum final density. Fig. 3 shows the different final densities that are obtained by infiltrating preforms with various initial densities, 60 % dense, 70 % dense and 80 % dense. The straight lines in the plot indicate the final density obtainable by filling of the pores by the melt without rearrangement of the particles. From comparison of the final densities achieved, it is clear that the densification due to rearrangement is significant for

the preform with 70 % density. The rearrangement process is significant because of the excellent wetting of the carbide particles by the molten metal and spontaneous infiltration along the grain boundaries of carbide agglomerates, similar to that seen in Fig. 2. With molten metal presumably present around each carbide grain, rearrangement and densification can take place easily. Clearly, there are quite a few factors that affect the rate of melt infiltration and also the extent of rearrangement, such as, effective capillary radius, the tortuosity of the pore channels and rigidity of the carbide skeleton from pre-sintering. A clear idea of the effect of these factors is discussed in the detailed analysis of the infiltration of molten aluminum in porous TiC [36,39].

The lower density of the cermet obtained by infiltration of the 80 % dense preform, as compared to infiltration of the 70 % dense preform, could also be due to some closed porosity that is not easily eliminated. In addition, the higher sintering temperature used for the processing of the preform could slow the kinetics of rearrangement due to a larger amount of carbide-carbide contacts. The 60 % dense preform, presumably, has a larger number of pores to be eliminated within the sintering duration thus, resulting in a low density cermet.

3.4. Comparison of Microstructures Obtained by Melt Infiltration versus Liquid Phase Sintering of Mixed Powders:

TiC-Fe40Al cermets can be processed by liquid phase sintering of pellets containing a mixture of Fe40Al and TiC powders. This was successful in the processing of the composites with carbide contents lower than 60 vol. % [7,8]. With an increase in the carbide volume fraction, higher density of the cermets can be obtained only upon a rearrangement of the particles aided by a solution-reprecipitation reaction. However, as shown in section 3.2, the solubility of TiC in liquid Fe40Al is very limited and thus significant rearrangement is not expected. The resulting low density is shown in Fig. 4, where cermets obtained by liquid phase sintering of mixed powders have a density equal to 90 to 97 % of the theoretical value for binder volume fractions varying from 0.1 to 0.3. On the other hand, melt infiltration allows processing of cermets to very high densities (> 97 % theoretical). The difference between the microstructures obtained by liquid phase sintering of mixed powders and melt infiltration of TiC preforms is clearly illustrated in Fig. 5. The Fe40Al powders (~ 40 μm) are large compared to the TiC (2-3 μm) powders and upon melting (aided by good wetting), the molten metal is wicked into the grains surrounding the original aluminide particle, leaving behind large pores. These pores cannot be eliminated due to the slow kinetics of a solution-reprecipitation reaction. This results in a porous and inhomogenous microstructure as shown in Figs. 5(d-f). During infiltration, no large pores need to be eliminated and rearrangement of particles is sufficient to densify the cermet. Comparison of Figs. 5(a-c) and 5(d-f) clearly show an improvement in the homogeneity of the microstructure obtained by melt infiltration. Figs. 6a and b show the typical microstructures, at a higher magnification, obtained for the melt infiltrated WC- and TiC-based cermets, with a binder volume fraction of 0.3. A continuous intermetallic phase is observed in these micrographs. The presence of a thin film of the intermetallic phase around all particles leads to a low TiC contiguity, a measure of the carbide-carbide contact in the composite. This has been observed to be a beneficial feature in the microstructure which can lead to higher strengths and improved fracture toughness [40].

Compositional analysis, using an energy dispersive spectrometer, showed that the ratio of the Fe content (58 at. %) to the Al content (38 at. %) in the binder phase was 1.52, almost equal to the initial composition. This indicates that during processing, the loss of Al due to evaporation is almost negligible. In the FeAl-TiC cermet, small amounts of Ti in the alloy binder (~1-2 at. %) and almost no Fe or Al in TiC were detected. No secondary phases were observed during examination in the SEM. In the Fe40Al-WC composite, tungsten concentrations in the binder were determined to be 5 at. % and this amount could be both from W dissolved in the iron aluminide and from very fine WC not observed by the SEM. Detailed TEM work would be

necessary to clarify the contributions. Concentrations of Fe and Al in WC were below the detectability limit and examination in the SEM did not reveal any secondary phases in the FeAl binder.

3.5. Mechanical Property :

Flexural strengths and chevron-notch fracture toughnesses of the composites were determined using a 3-point bend testing set-up. For the chevron-notched specimens, since fracture occurred in a stable manner, the energy dissipated during the fracture of the sample, per unit crack area (denoted as G) was obtained by integrating the area under the load-displacement curve. The fracture toughness was then obtained using the following equation:

$$K_q = [E \cdot G / (1-\nu^2)]^{1/2}$$

where E is the elastic modulus of the composite and ν is Poisson's ratio (taken to be 0.2 in our case). The plane strain elastic modulus, E', was calculated from the following equation for a two-phase composite given in Ref. [41].

$$E' = [(cE_pE_m + E_m^2)(1 + c)^2 - E_m^2 + E_pE_m]/[(cE_p + E_m)(1 + c)^2]$$

where $c = (1/V_p)^{1/3} - 1$ with $V_p + V_m = 1$

with V_p and V_m are the volume fractions of carbide particles and the intermetallic phase, respectively. E_p is the elastic modulus of the carbide phases (TiC - 430 GPa [1], WC - 696 GPa [42]) and E_m denotes the elastic modulus of iron aluminide (180 GPa [43]).

Table 2a reports the typical values for the fracture toughness, flexure strength and hardness for the iron aluminide bonded TiC cermets. The values for a commercial Ni-bonded TiC cermet are also shown for comparison. Table 2b summarizes the values for the fracture toughness obtained for the Fe40Al-WC cermets. Results of the hardness and the bend strength values are reported in detail elsewhere [14].

TABLE 2

(A) Selected mechanical properties of Fe40Al-TiC cermet and a commercially available cermet.

Binder composition (at. %)	Binder vol. %	Carbide compo -sition & wt. %	Hardness	Bend Strengths (in MPa)	Fracture Toughness (MPa· $m^{1/2}$)
Fe-40Al	40 vol. %	TiC - 55 wt. %	83.5 R_A	1058 MPa	21.4 (2 tests)
Fe-40Al	30 vol. %	TiC - 65 wt. %	84 R_A	1034 MPa	18 (3 tests)
Fe-40Al	20 vol. %	TiC - 76.5 wt. %	87 R_A	750 MPa	12.7 (3 tests)
[a]Ni-16Mo	21 vol. % (=33 wt. %)	TiC - 58 wt % NbC - 6 wt % WC - 3 wt %	89 R_A	1700 MPa	10.6

a - Ref. 1

(B) Fracture toughness of Fe40Al-WC cermets

Binder Composition (at. %)	Binder (vol. %)	Fracture Toughness ($MPa \cdot m^{1/2}$)
Fe-40Al	30	10.7 (3 tests)
Fe-40Al	20	10.6 (2 tests)
Fe-40Al	15	7.9 (2 tests)

For the iron aluminide bonded TiC cermets, the hardness of the cermet with 20 vol. % binder is comparable to the commercially available cermet, however 3-point bend strengths are much lower. Significant improvements in the bend strengths values are needed for heavy duty cutting applications. However, the strengths are sufficiently high for static wear applications in corrosive atmospheres.

Although iron aluminides are considered to be brittle, relatively high values for the fracture toughness of Fe40Al-TiC cermets are obtained. The fracture toughness of the TiC cermet with 20 vol. % iron aluminide is higher than that of Ni-bonded TiC cermets for a similar volume fraction, although the Ni binder is expected to fracture in a ductile manner. Relative to toughnesses of FeAl-TiC cermets, the values for Fe40Al-WC cermets are modest and the reasons are not quite clear. However, the high fracture toughness value obtained in FeAl-TiC cermets suggest that the behavior of iron aluminide as thin ligaments could be different. A possible explanation for the mechanical behavior of iron aluminide in the cermets is suggested below.

The fractured surface of a chevron-notched Fe40Al-TiC test specimen, with 30 vol. % Fe40Al, is shown in Fig. 7. From the micrograph, it is very clear that there is significant debonding at the carbide/intermetallic interface and deformation of the iron aluminide phase suggests ductile behavior of the intermetallic. Observations of fracture surfaces in intermetallic-ceramic composites in previous investigations [7,13,14] have also indicated that intermetallics when used as a binder phase in cermets could show some ductility.

The predominant contribution to increased toughness of composites of brittle materials and ductile reinforcements is the plastic work expended upon elongation of the ductile ligaments to failure between the crack surfaces, within the crack tip bridging zone [44,45]. Previous studies, particularly in WC-Co composites, have suggested that the in-situ flow stress of Co is likely to be several times higher than its bulk flow stress value [44,45]. The increase in the flow stress depends upon the work hardening coefficient, the reinforcement ductility and the extent of interfacial debonding [45]. As shown in Fig. 7, debonding at the carbide/Fe40Al interface is evident. From Ashby and Banister's model experiments, it is clear that weak interfacial bonding may result in much higher energy absorption, and therefore higher toughening, than strong interfacial bonding. In addition, although cleavage fracture is a predominant fracture mode for bulk Fe40Al single crystals [46], it is not the case for the fracture of the Fe40Al ligaments in these composites, as seen in Fig. 7. This suggests that for small ligament sizes, the distances available for dislocation pile-up are not large enough to result in a cleavage fracture. Further systematic studies are underway to better understand the role of the intermetallic phase in improving the toughness of these composites, especially towards identifying the correlation between the scale of the iron aluminide ligaments and their mode of fracture.

In addition, observations of the microstructure in liquid phase sintered WC-Co cermets have shown that the grain size of the Co in the composite is on the order of about 1 mm [47,48]. Assuming that this is the case in these cermets too, each deforming ligament (less than 10 μm

wide) essentially acts as a single crystal during the fracture process. Thus, contribution from intergranular failure, resulting due to weakness in grain boundaries, is absent.

3.6. Oxidation resistance:

Since bulk iron aluminides have superior oxidation resistance, a simple comparison study was conducted to determine its effectiveness when present as a binder in the composites. The most commonly used cemented carbide, WC/Co, was used as a basis for the comparison. Fig. 8 shows the results from exposure to air at 900 °C for a day. It is evident that iron aluminides provide significant resistance to oxidation of the cermets.

4.0. SUMMARY

In this investigation, fully dense WC- and TiC-based cermets, with iron aluminide (Fe-40 at. % Al) as a binder, was processed by pressureless melt infiltration. For carbide contents greater than 70 vol. %, it was demonstrated that this technique allows fabrication of cermets to higher densities than through liquid phase sintering of mixed powders. The later approach was not successful due to a low solubility of the carbides in liquid Fe40Al at 1450 °C. The solubility limits were determined by phase equilibria calculations in the multicomponent system using the Thermocalc™ program. Liquid Fe-40 at. % Al in equilibrium with graphite dissolves about 5 at. % carbon and 1 at. % tungsten. In the Fe-Al-Ti-C system, molten Fe-40 at. % Al in equilibrium with $Ti_{0.512}C_{0.488}$ and graphite, dissolves 4.9 at. % carbon and 64 atomic ppm titanium. The carbide contents in these composites varied from 70 to 90 vol. %. Specimens with 30 vol. % intermetallic exhibited bend strengths of 1034 MPa, fracture toughness of 18 $MPa \cdot m^{1/2}$ and a Rockwell (R_A) hardness of 83.5. The Fe40Al-WC specimens with 30 vol. % Fe40Al had a bend strength of 1.4 GPa, fracture toughness of 10.6 $MPa \cdot m^{1/2}$ and a Rockwell (R_A) hardness of 88. The hardness values are comparable to those obtained for the commercially available WC-Co cermets. SEM observations of the fracture surface suggest that the high values for fracture toughness could be due to a ductile behavior of the intermetallics when present as thin, bridging ligaments in the composites. Improvements in bend strengths may be possible by controlling the grain size and by modifications of the Fe40Al/carbide interface strengths. In conclusion, the properties evaluated in this study indicate that these cermets could be beneficial in a variety of wear applications.

ACKNOWLEDGMENTS

The authors would like to thank Dr. Ellen Sun and Dr. Craig Blue for a very thorough review of the manuscript. This research is sponsored by the Laboratory Directed Research and Development Program of the Oak Ridge National Laboratory, and by the Division of Materials Sciences, U.S. Department of Energy, under Contract No. DE-AC05-96OR22464 with Lockheed Martin Energy Research Corp. This research was also supported in part by an appointment to the ORNL Post-Doctoral Research Associates Program administered jointly by the ORISE and ORNL.

REFERENCES

1. A.T. Santhanam, P. Tierney and Hunt, J.L., in Metals Handbook , ASM International, **2** (1990) 950.

2. E.A. Almond and B. Roebuck, Mat. Sci. and Engg., **A105/106** (1988) 237.

3. B. Roebuck, E.G. Bennett, and E.A. Almond, Int. J. Refract. Hard Met., **3** (1984) 35.

4. R.K. Viswanadham and P.G. Lindquist, Mett. Trans., **18A** (1987) 2163.

5. R.K. Viswanadham and P.G. Lindquist, Mett. Trans., **18A** (1987) 2175.

6. J. Wambold, in Cermets. Eds. J.R. Tinklepaugh and W.B. Crandall, Reinhold Publishing Corporation, 122-129, 1960.

7. J.H. Schneibel and C.A. Carmichael, in *SinteringTechnology,* (eds.), R.G. Cornwall, G.L. Messing and R.G. German, Marcel Dekker Inc., 253-260, 1996.

8. J.H. Schneibel, C.A. Carmichael, E.D. Specht and R. Subramanian, Intermetallics 5, 61-67, 1997.

9. T.N. Tiegs, K.B. Alexander, K.P. Plucknett, P.A. Menchhofer, P.F. Becher and S.B. Waters, Mat. Sci. and Engg., A209 243-247 1996.

10. P.F. Tortorelli and J.H. DeVan, in *Processing, Properties and Applications of Iron Aluminides*, J.H. Schneibel and M.A. Crimp, eds., TMS, Warrendale, PA., 257, (1994).

11. C.G. McKamey, J.H. DeVan, P.F. Tortorelli and V.K. Sikka, *J. Mater. Res.*, **6** , 1779 (1991).

12. J.H. DeVan, in *Oxidation of High-Temperature Intermetallics*, T. Grobstein and J. Doychak (eds.), TMS, 107 (1989).

13. R. Subramanian, J.H. Schneibel, K.B. Alexander and K.P. Plucknett, Scr. Mater., 35, 583 1996.

14. R. Subramanian and J.H. Schneibel, J. Intermetallics, 1996 (accepted for publication).

15. K.P. Plucknett, P.F. Becher and R. Subramanian, J. Mat. Sci. letters., 1996 (submitted for publication).

16. K.A. Semlak and F.N. Rhines, Trans. of the Met. Soc. of AIME, **212**,325-331, 1958.

17. D. Muscat, K. Shanker and R.A.L. Drew, Mater. Sci and Tech. 8, 971-976 1992.

18. W.D. Wolf, L.F. Francis, C-P. Lin and W.H. Douglas, J. Am. Ceram. Soc., 76[10] 2691- 94 1993.

19. H. Nakanishi, Y. Tsunekawa, M. Okumiya and N. Mohri, J. Mat.Sci. Letters, 1313-1315, 1993.

20. T.W. Clyne and J.F. Mason, Metall. Trans., 18A, 1519-1530, 1987.

21. J. Rodel, H. Prielipp, N. Claussen, M. Sternitzke, K.B. Alexander, P.F. Becher and J.H. Schneibel, Scripta Metall. Mater., 33 843, 1995.

22. W.B. Hillig, R.L. Mehan, C.R. Morelock, V.J. Decarlo and W. Laskow, Am. Cer. Soc. Bull. 54(12), 1054- 1056, 1975.

23. W.B. Hillig, Am.Cer. Soc. Bull., 73(4), 56-62, 1994.

24. M.K. Aghajanian, J.P. Biel and R.G. Smith, J. Am. Ceram. Soc., 77(7), 1917-1920, 1994.

25. R.E. Loehman, K. Ewsuk and A.P. Tomsia, J. Am. Ceram. Soc., 199?.

26. M. C. Breslin, J. Ringnalda, L. Xu, M. Fuller, J. Seeger, G. S. Daehn, T. Otani, and H. L. Fraser, Mat. Sci. & Eng. A195, 113 (1995).

27. M.A. Pietzka and J.C. Schuster, J. Phase Equilibria, 15(4) 1994.

28. K.C. Hari Kumar and V. Raghavan, J. Phase Equilibria. 275-286 12(3) 1991.

29. M. Palm and G. Inden, J. Intermetallics, 3 1995 443-454.

30. H. Ohtani, T. Tanaka, M. Hasebe and T. Nishizawa, CALPHAD 12(3) 225-246 1988.

31. M. Hillert, CALPHAD, 4(1), 1-12, 1979.

32. K. Balasubramanian, A. Kroupa and J.S. Kirkaldy, Met. Trans., 23A 709-727, 1992.

33. G.P. Dmitrieva, N.A. Razumova and A.K. Shurin, Sov. Powder Metall. Met. Ceram, 23, 2(254), 159-162, 1984.

34. A.F. Guillermet, Metall. Trans. 20A (5) 935-956. 1989.

35. I. A. Aksay, C.E. Hoge, and J.A. Pask, J. of Phys. Chem., 78(12) 1178, 1974.

36. D. Muscat and R.A.L. Drew, Metall. Trans. 25A 2357-2370, 1994.

37. D. Moskowitz and M. Humenik, in Modern Development in P/M 3, 83-94, 1966.

38. E.W. Washburn, Phys. Rev., 27(3) 273-283, 1921.

39. D. Muscat, R.L. Harris and R.A.L. Drew, Acta. Metall. 42(12) 4155-4163, 1994

40. J. Gurland and P. Bardzil, *Trans. AIME, J. of Metals,* **203** 311 (1955).

41. K.S. Ravichandran, *Acta. Metall. Mater.*, **42**(4), 1113 (1994).

42. P.T.B. Shaeffer, ASM Handbook, **2** (1990) 804.

43. J.H. Schneibel and M.G. Jenkins, Scr. Metall. Mater., **28** (1993) 389.

44. L.S. Sigl and H.F. Fischmeister, Acta Metall., **36(4)** (1988) 487.

45. M.F. Ashby, F.J. Blunt and M. Bannister, Acta. Metall., **37(7)** (1989) 1847.

46. Gaydosh, D.J., Draper, S.L., Noebe, R.D., and Nathal, M.V., Mater. Sci. and Eng., **A150**, (1992) 7.

47. O. Rüdiger and H.E. Exner, Pow. Metall. Int., **8(1)** (1976) 7.

48. J. Willbrand and W. Weiland, Int. J. Powd. Metall., 8 (2), 89-93 (1972).

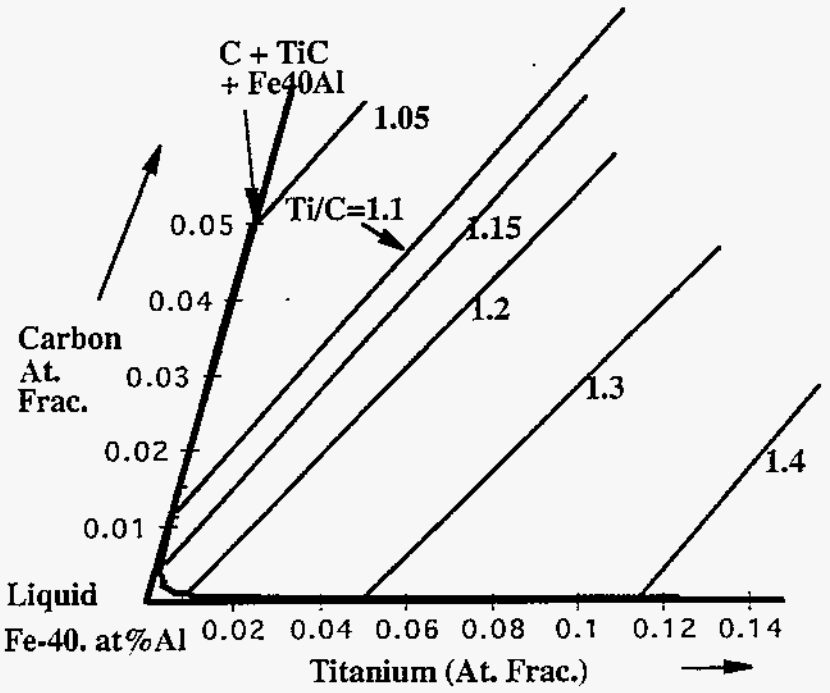

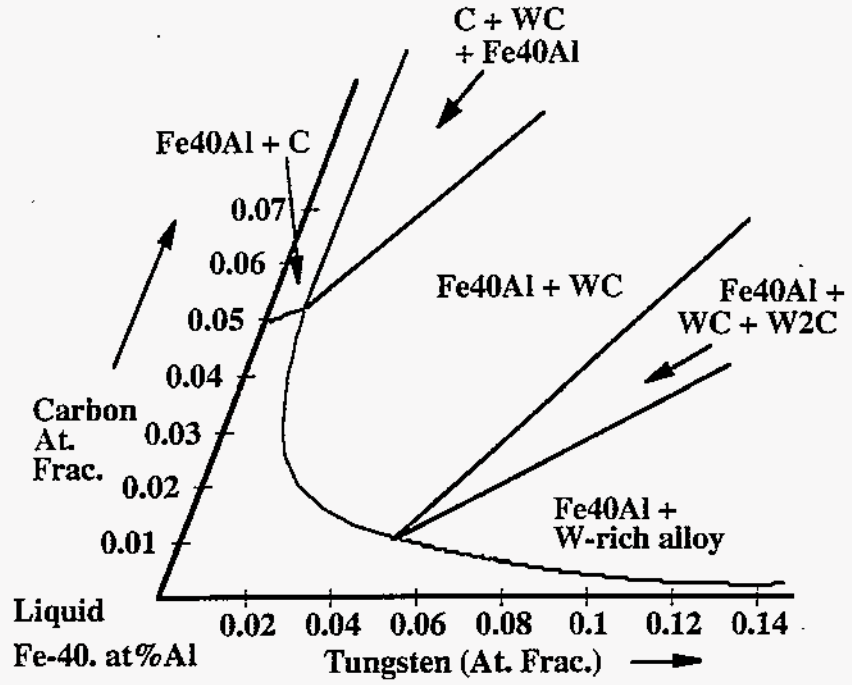

Fig. 1: Plot of the Fe-Al-Ti-C and Fe-Al-W-C sections at 1450 °C showing the solubility of W, Ti and C in liquid iron aluminide (Fe-40 at. % Al).

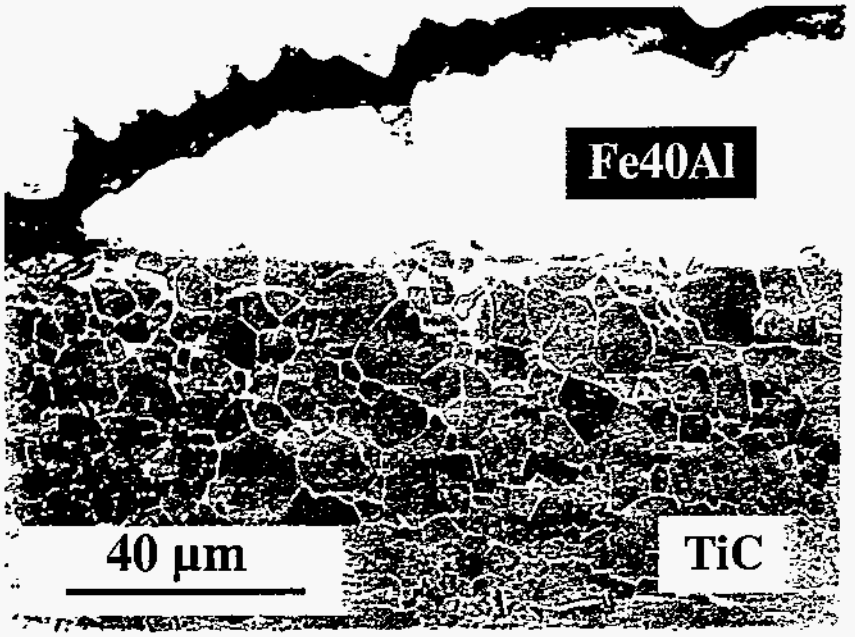

Fig. 2: Liquid Fe40Al wets dense TiC (97 % theoretical density) and penetrates along the carbide grain boundaries.

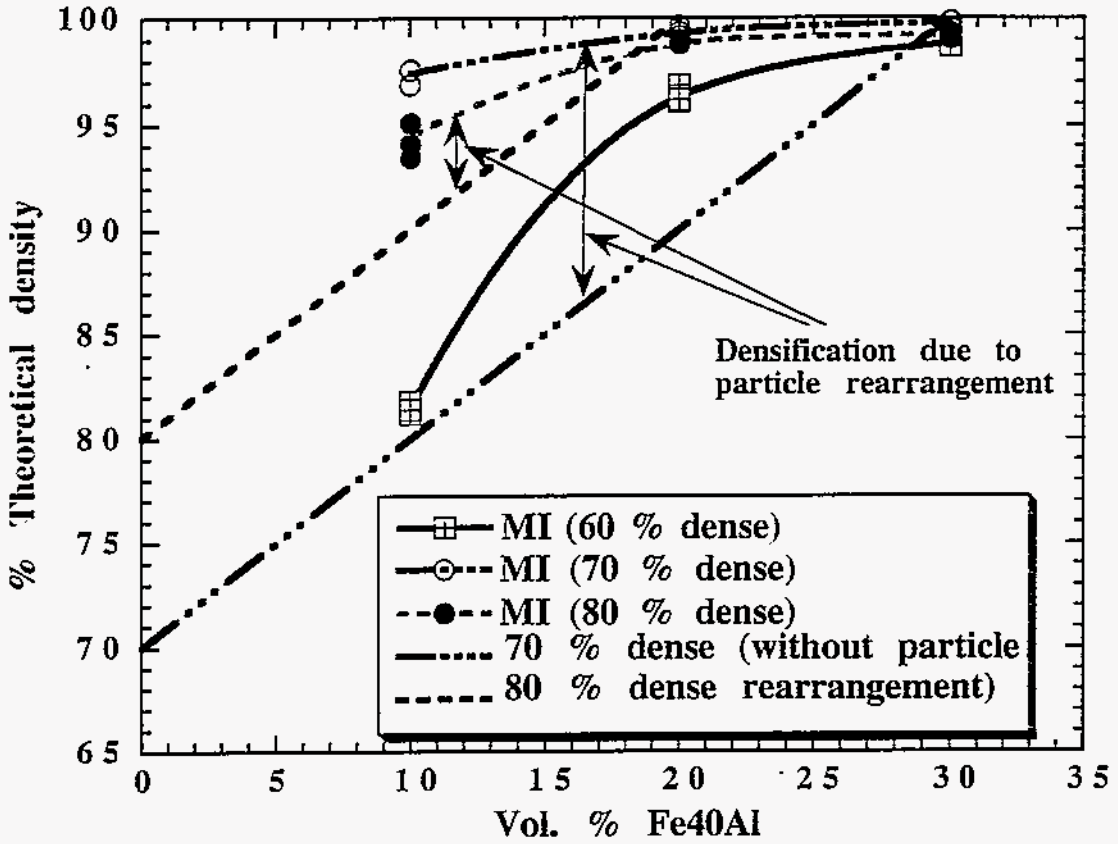

Fig. 3: Effect of the TiC preform density on the final density of the Fe40Al/TiC cermet processed by melt infiltration.

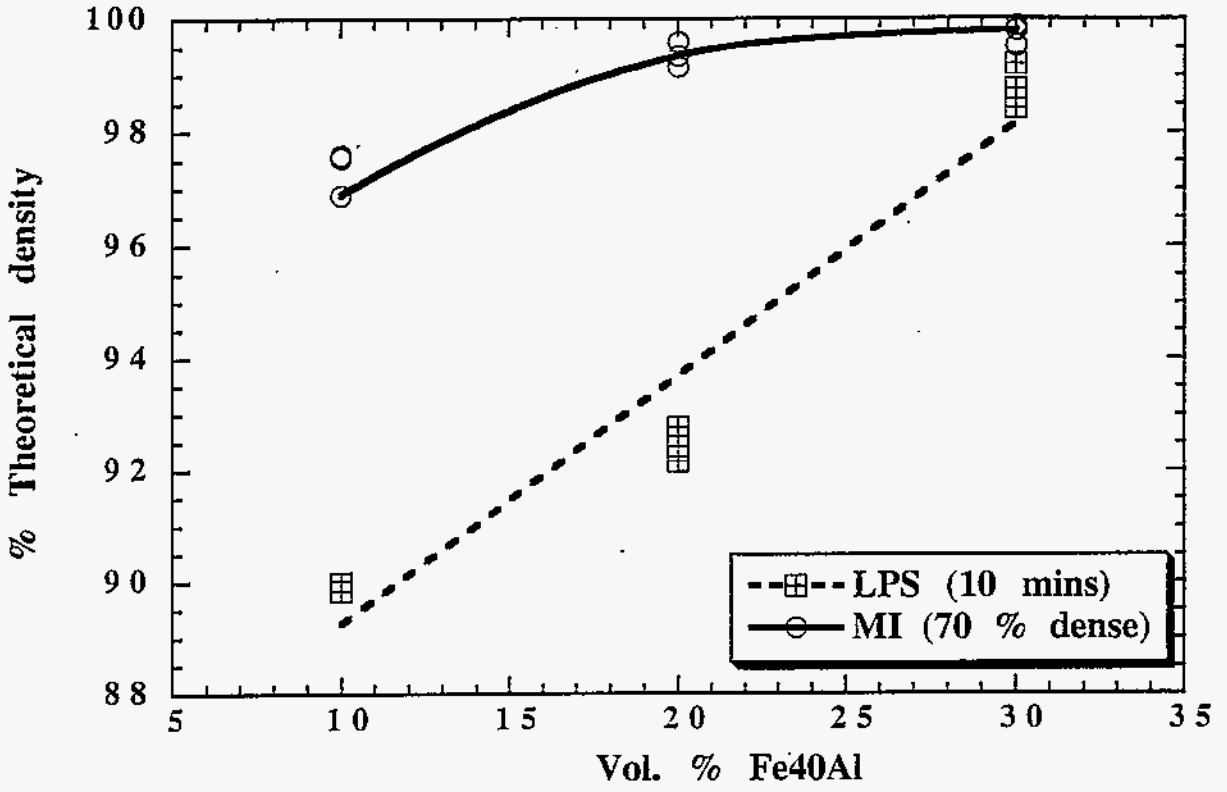

Fig. 4: Comparison of the final densities of Fe40Al/TiC cermets processed by melt infiltration (MI) and liquid phase sintering of mixed powders (LPS).

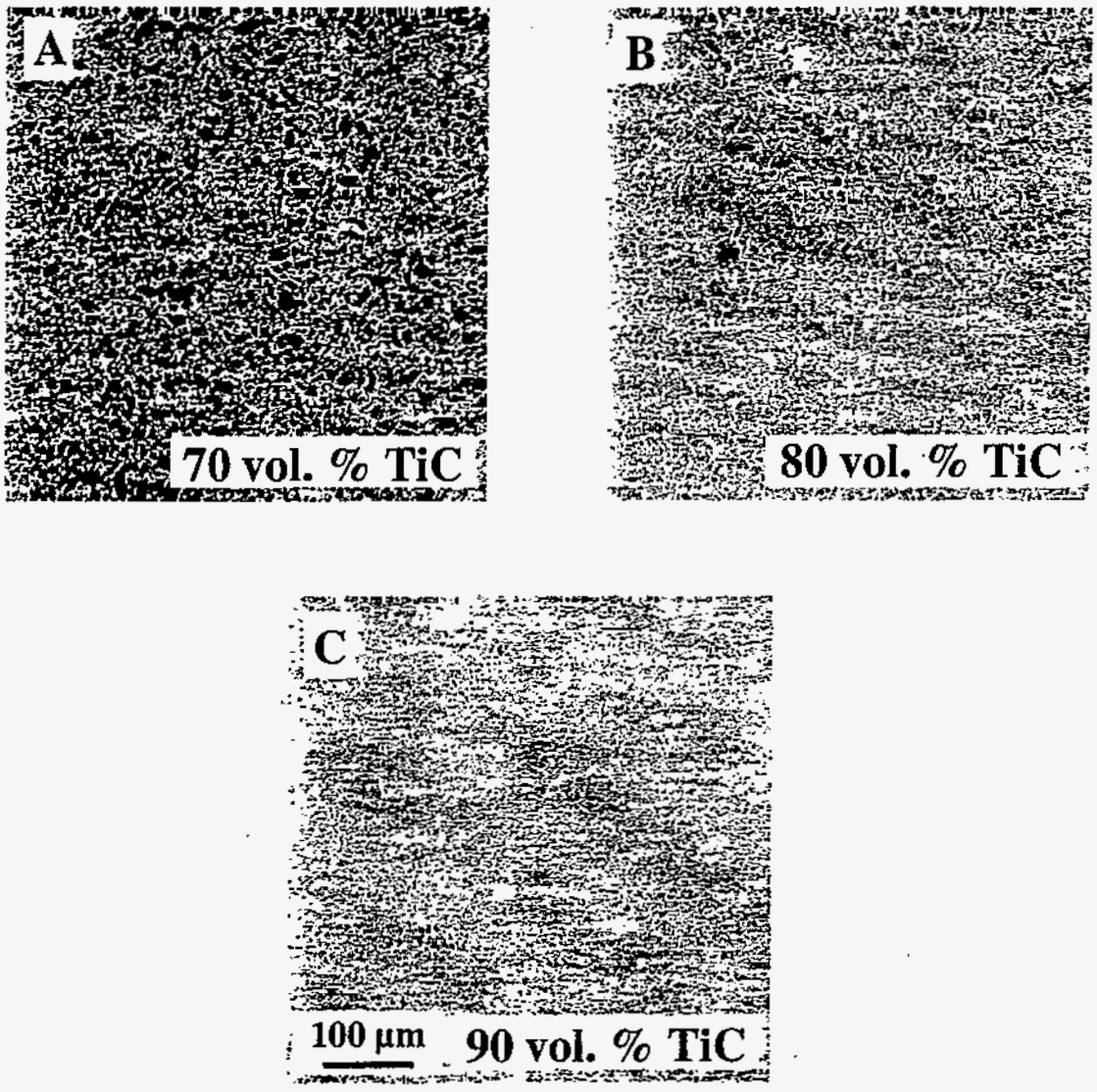

Fig. 5: Comparison of microstructures obtained by melt infiltration as shown in A to C versus those obtained by liquid phase sintering of mixed powders as shown in D to F for different volume fractions of TiC in the Fe40Al/TiC cermet.

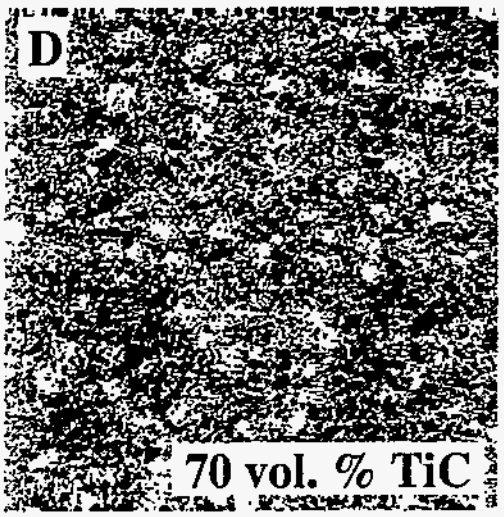
D
70 vol. % TiC


E
80 vol. % TiC

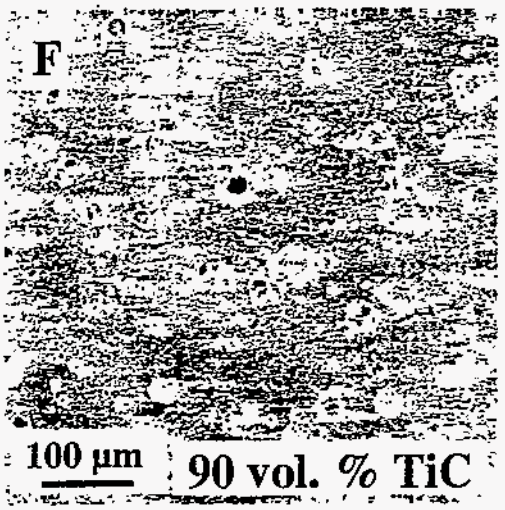
F
100 µm
90 vol. % TiC

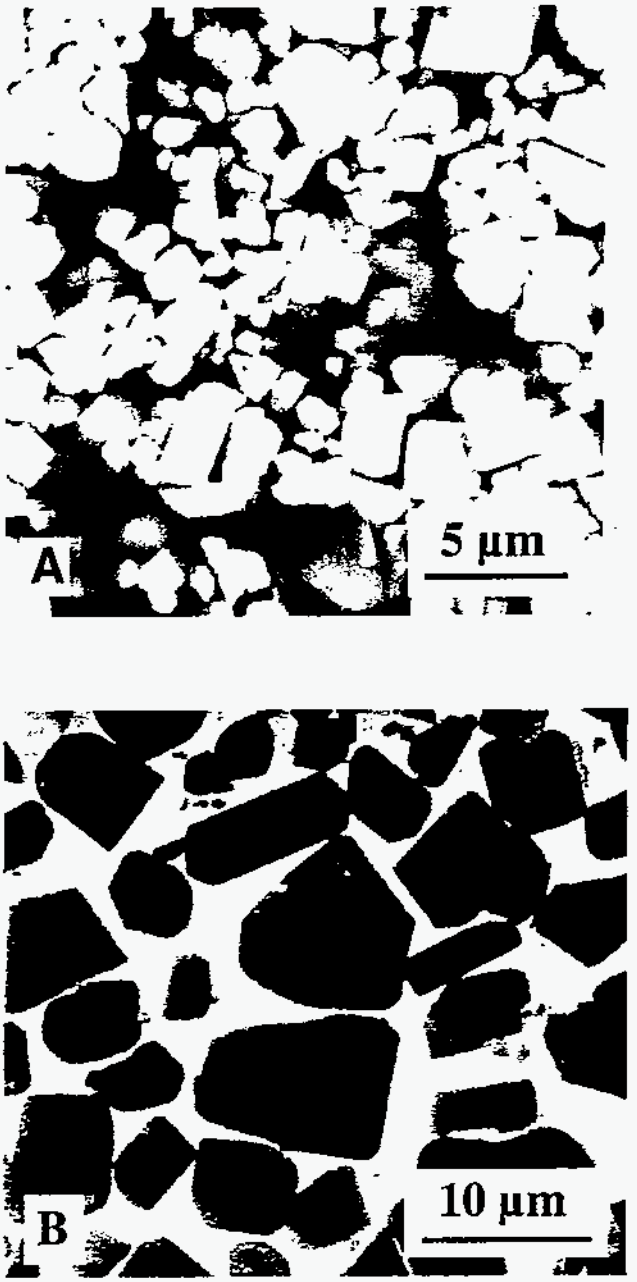

Fig. 6: Typical microstructures of the FeAl bonded (a)WC and (b) TiC cermets with 30 vol. % iron aluminide.

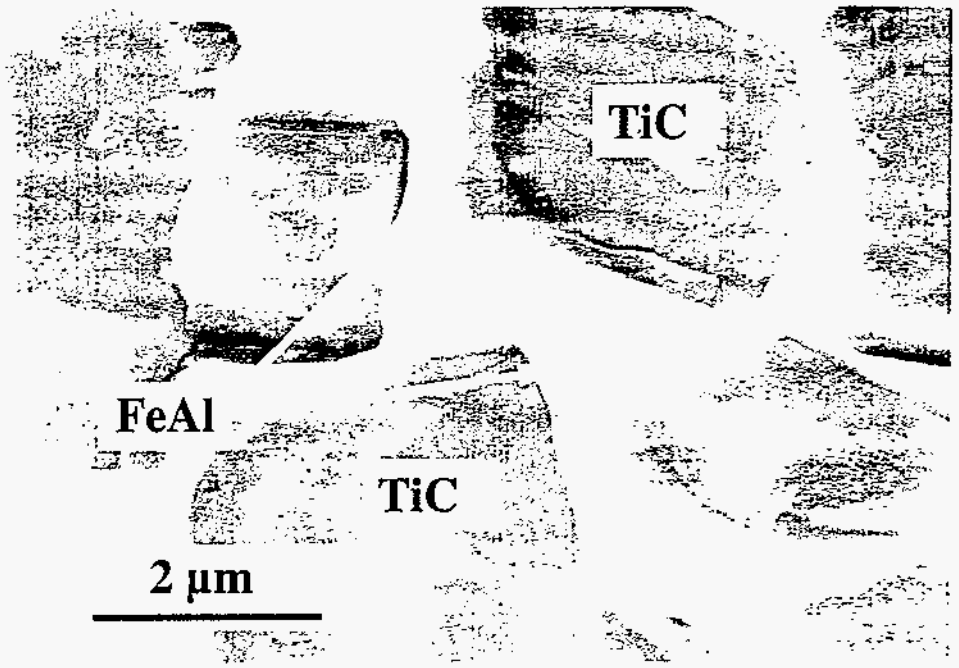

Fig. 7: Fracture surface of FeAl bonded TiC cermet with 30 vol. % iron aluminide.

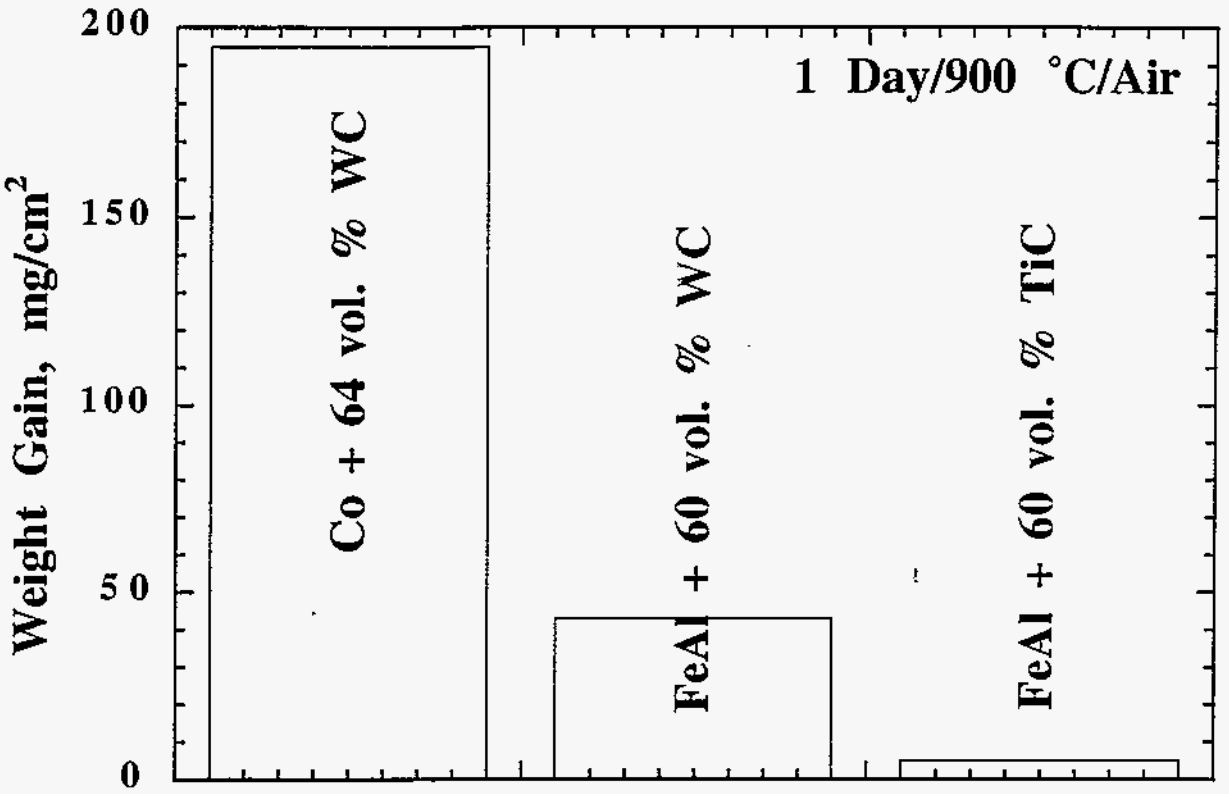

Fig. 8: Comparison of oxidation resistances of aluminide bonded cermets with WC-Co cermets.